Small-Angle X-ray Scattering by Dilute Solution of Bisphenol A Polycarbonate during Adding Antisolvent CO_2

Dan Li,[†] Buxing Han,*[,†] Qing Huo,[‡] Jun Wang,[§] and Baozhong Dong[§]

Center for Molecular Sciences, Institute of Chemistry, Chinese Academy of Science, Beijing 100080, China; Chemical Engineering College, Beijing Union University, Beijing 100023, China; and Institute of High Energy Physics, Chinese Academy of Science, Beijing 100039, China

Received September 26, 2000; Revised Manuscript Received April 17, 2001

ABSTRACT: Small-angle X-ray scattering (SAXS) was used to investigate the dimension, shape, and microstructure of bisphenol A polycarbonate (PC) of narrow distribution in tetrahydrofuran (THF) in the course of adding gaseous antisolvent CO_2 at 308.15 K and at pressures up to 2 MPa. The weight-average molecular weights (M_w) of the polymer samples were 1.4×10^4, 1.8×10^4, 2.4×10^4, and 2.9×10^4, and the concentration of the polymer in the solution ranged from 1.2×10^{-3} to 9.1×10^{-3} g/cm^3. The second virial coefficient A_2 and the radius of gyration $\langle R_g^2 \rangle^{1/2} \equiv R_g$ were found to decrease with the increasing of the antisolvent pressure. The M_w of the PC chain was scaled to the R_g of the polymer chain as $M_w \propto R_g^{d_R}$ (d_R = 2.17, 2.38, 2.56, 2.74, and 2.95) for different antisolvent CO_2 pressures (P = 0, 0.5, 1, 1.5, and 2 MPa), suggesting that the PC chain has a fractal structure in the presence antisolvent CO_2. Self-similar structure behavior was also observed with a detailed analysis of the particle scattering factor $P(q)$ (angular dependence of the scattered light), and the fractal dimensions d_f at 0, 0.5, 1.0, 1.5, and 2 MPa are 2.14, 2.35, 2.53, 2.70, and 2.92, respectively. All of these revealed a large effect of antisolvent pressure or the solubility of CO_2 in the solution on PC structure. Increase of fractal dimension (d_R or d_f) from 2.17 to 2.95 indicates that the polymer chain changes from a swollen coil to a rather dense globule in the course of adding antisolvent CO_2.

Introduction

The use of supercritical fluids (SCFs), especially supercritical carbon dioxide (SC CO_2), as a medium for fine particle formation is a rapidly developing field of research.[1] The possibility of obtaining solvent-free microparticles with narrow size distribution makes this technology especially attractive. The gaseous antisolvent (GAS) process is one of the most important techniques.[2] The basis of the GAS technique[3] is the fact that the fluids at a dense gas state are generally soluble in organic solvents and in solutions of these solvents with crystallizable solutes. Dissolution of GAS causes a volumetric expansion of the solvent and lowers its solvent power and thus forces the solute to precipitate. Because of the high and uniform degree of supersaturation, small particles with a narrow size distribution are expected. Moreover, it is possible to extract all the solvent in the gas phase and to obtain solvent-free product. To date, GAS processes have been successfully used in the recrystallization of organic solids,[4,5] the fractionation of natural products,[6,7] and the preparation of ultrafine particles.[3,8−18] Since only a few kinds of polymers have been found to be soluble in compressed CO_2,[19] it can be used as an environmentally benign antisolvent for processing most polymers.[11−18] The polymer morphology can be tailored by temperature and pressure since the solubility of a gas in an organic solvent can be tuned by pressure and temperature. It is obvious that investigation of the effect of gas antisolvent on the polymer conformation has both theoretical and practical importance.

Small-angle X-ray scattering (SAXS) has been proved to be a particular useful method to study polymer conformation, especially in dilute solutions,[20−24] and it is also a direct method to study fractal structures on the basis of the scattered intensity and the size dependence of the molar mass.[25−28] Schulz and Horbach[29] remarked that the bisphenol A polycarbonate, hereafter referred to as polycarbonate (PC), belonged, in qualitative terms, to an intermediate class between flexible and semiflexible chains. PC is soluble in some solvents, such as tetrahydrofuran (THF), dichloromethane (DCM), chloroform ($CHCl_3$), and ethylene dichloride (EDC). We are very interested in studying the change of conformation and microstructure of polymers in the course of adding GAS and hope to be able to relate these properties with the macroscopic properties of the products of GAS processes. In this work, we investigated properties of PC/THF solution in the course of adding GAS CO_2 using SAXS. To avoid the complications related to intermolecular interactions, our experiments deal mainly with the dilute solutions. We focused on (1) the investigation of the phase behavior of the PC/THF/CO_2 system; (2) the thermodynamics of polymer solution with emphasis on the fundamental parameters, such as the radius of gyration R_g and the second virial coefficient A_2 over a wide range of antisolvent pressure; and (3) the structure of PC chain by the scatter factor $P(q)$. The analysis of the obtained polymer chain scattering factor $P(q)$ allowed extraction of information on the structure properties of PC chain as a function of antisolvent CO_2 pressure by fractal theory.

Experimental Section

Materials. PC samples of different molecular masses PC-1 (1.4×10^4), PC-2 (1.8×10^4), PC-3 (2.4×10^4), and PC-4 (2.9×10^4) with narrow molecular weight distribution were kindly supplied by the State Key Laboratory of Polymer Physics and

[†] Institute of Chemistry, Chinese Academy of Science.
[‡] Beijing Union University.
[§] Institute of High Energy Physics, Chinese Academy of Science.
* To whom the correspondence should be addressed. E-mail hanbx@pplas.icas.ac.cn; Tel (8610)-62562821; Fax(8610)-62559373.

10.1021/ma001671k CCC: $20.00
Published on Web 06/05/2001

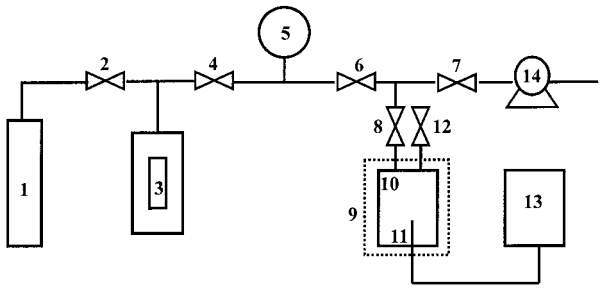

Figure 1. Schematic diagram of the apparatus for SAXS experiments of polymer solutions in GAS process: (1) gas cylinder; (3) high-pressure pump; (5) pressure gauge; (9) SAXS spectrometer; (10) high-pressure SAXS cell; (11) thermometer; (13) temperature controller; (14) vacuum pump; (2), (4), (6), (7), (8), (12) valves.

Chemistry, Institute of Chemistry, Chinese Academy of Sciences. The solvent THF (A.R. grade) was produced by Beijing Chemical Factory and used without further purification. The PC/THF solutions were prepared by the gravimetric method. The original concentrations (CO_2-free) of the solutions, C_0, in our study were 1.261×10^{-3}, 4.338×10^{-3}, 6.388×10^{-3}, and 9.124×10^{-3} g/cm^3.

Phase Behavior. The apparatus and procedures for measuring the volume expansion coefficient (V_e) and the cloud point pressure (P_c) of the PC/THF/CO_2 system were similar to that reported previously.[30] Briefly, the apparatus consisted mainly of a 30 mL stainless steel optical cell, a magnetic stirrer, a constant temperature water bath, a pressure gauge, a gas cylinder, and a high-pressure pump. In a typical experiment, a suitable amount of PC/THF solution was loaded into the optical cell, and the cell was stabilized at the desired temperature. CO_2 was charged into the cell using the high-pressure pump until suitable pressure was reached. When equilibrium was reached, the pressure remained constant with time, and the volume of solution was known by reading the graduations on the cell. Some polymer molecules precipitated when the equilibrium pressure was high enough, which could be seen clearly through the windows of the optical cell. The cloud pressure, P_c, which was defined as the pressure at which the polymer begins to precipitate, was determined.

The solubility of CO_2 in the solution was also determined by the high-pressure vapor−liquid equilibrium apparatus in our laboratory, which was described in detail previouly.[31] The solubility data were accurate to ±2%.

SAXS Measurement. The schematic diagram of the experimental setup for the SAXS study is shown in Figure 1, which is similar to that of the on-line FT-IR measurement.[32] The apparatus consisted mainly of (1) gas cylinder; (2) high-pressure pump, (5) digital pressure gauge, (9) SAXS spectrometer, (10) high-pressure SAXS cell, (11) thermometer, (13) temperature controller, and (14) vacuum pump and valves and fittings of different kinds. The pressure gauge consisted of a transducer (FOXBORO/ICT) and an indicator. The temperature-controlled SAXS cell was made of stainless steel with two diamond windows of 8 mm diameter and 0.4 mm thick. The cell body was wrapped with an electric heater and heat-insulated ribbon. The X-ray path length of the cell was 1.5 mm, and the internal volume of the cell was 2.7 cm^3. There was a small magnetic stirrer in the cell to stir the fluids before the SAXS measurements, so that the equilibrium could be reached in a shorter period of time. The insulated cell was electrically heated to ±0.1 K of the desired temperature using a temperature controller with a platinum resistance temperature probe (model XMT, produced by Beijing Chaoyang Automatic Instrument Factory).

SAXS experiments were carried out at Beamline 4B9A at the Beijing Synchrotron Radiation Facility, using a SAXS apparatus constructed at the station.[33] The experiments had an angular resolution of better than 0.5 mrad with this setting. The data accumulation time was 2 min. The angular range was chosen to provide data from $q = 0.005$ Å^{-1} to $q = 0.15$ Å^{-1}, where the magnitude of scattering vector $q = 2\pi \sin \theta/\lambda$, with θ and λ being respectively the scattering angle and incident X-ray wavelength of 1.54 Å. The distance between the sample chamber and the detector was 1.52 m. Two ionization chambers were used to measure the sample transmission. Background scattering from the slit collimator, the solvent, and the residual air path between the vacuum chamber and the detector was measured and subtracted. It should be mentioned that the background solvent scattering is that scattered from solvent + antisolvent, so that we could obtain the information on polymer chain. Excess SAXS scattering from PS solute was also corrected for incident beam decay and sample transmission.

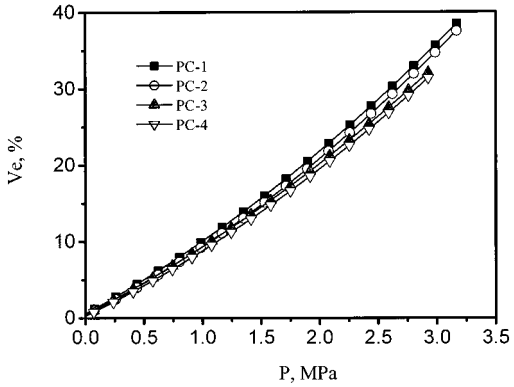

Figure 2. Dependence of volume expansion coefficient (V_e) on antisolvent CO_2 pressure for four samples with original solution concentration C_0 of 1.261×10^{-3} g/cm^3.

Before the experiment, the SAXS cell was flushed with CO_2, and then a suitable amount of PC/THF solution was filled into the cell. CO_2 was charged into the cell with stirring at the desired temperature. Once equilibrium was reached, the cell was connected to the apparatus and the small-angle X-ray scattering was recorded.

Results and Discussion

Phase Behavior. The solution is expanded by the dissolved CO_2, and the concentration of CO_2 in the solution is directly related with the volume expansion coefficient (V_e), which is defined as $(V - V_0)/V_0$, where V_0 and V are the volume of solution before and after dissolving antisolvent CO_2. In this work, the V_e of PC/THF (PC-1, PC-2, PC-3, and PC-4) solutions was determined at 308.15 K and at different CO_2 pressures. The original (CO_2-free) concentrations C_0 of the solutions were 1.261×10^{-3}, 4.338×10^{-3}, 6.388×10^{-3} and 9.124×10^{-3} g/cm^3. The V_e experiments were repeated at least three times, and the reproducibility was better than ±1%. The cloud point pressures (P_c) of the solutions were also measured. As an example, Figure 2 shows the V_e of PC/THF solutions of the four PC samples at $C_0 = 1.261 \times 10^{-3}$ g/cm^3. The figure shows that the effect of molecular weight (M_w) of PC on V_e is very limited. Experiments also showed that the concentration of the polymer in the solution does not affect the V_e considerably at our experimental conditions. Figure 3 shows the P_c for the four samples at different C_0. As expected, the P_c decreases with the original concentration of the solution and M_w. The V_e data in Figure 2 allowed us to determine how much solution should be charged into the SAXS cell. On the basis of the Pc data in Figure 3, we could select the experimental conditions to avoid the precipitation of PC in the SAXS experiments.

In this work, the solubility of CO_2 in the polymer solutions was determined at 308.15 K. Figure 4 shows

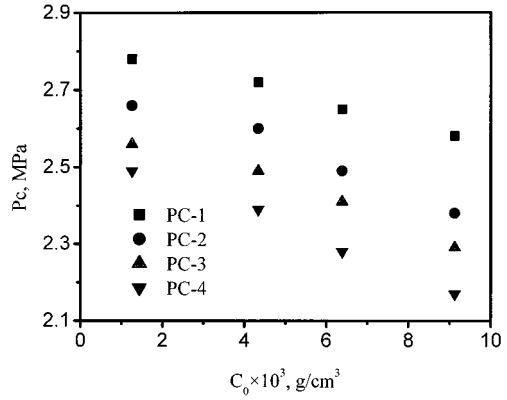

Figure 3. Effect of original concentration of solution C_0 on the cloud point pressures (P_c) for four PC samples at 308.15 K.

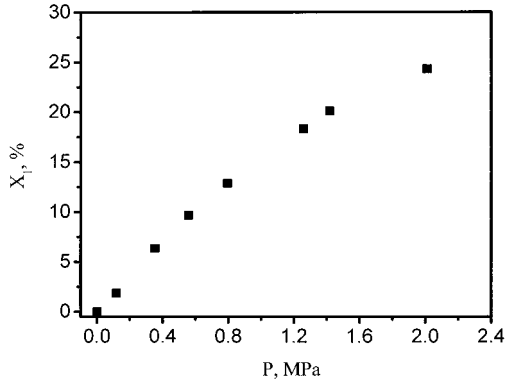

Figure 4. Solubility of CO_2 in PC-1/ THF solution ($C_0 = 1.261 \times 10^{-3}$ g/cm^3) at 308.15 K and different pressures.

the solubility of CO_2 in PC-1/THF solution with a C_0 of 1.261×10^{-3} g/cm^3. X_1 in the figure is the mole fraction of CO_2 in the solution. The solubility at other C_0 was also determined, and the results indicate that the effect of C_0 on the solubility is not considerable. This is easy to understand because the concentration of PC in the solutions is very low.

THF is a good solvent for PC, and CO_2 is an antisolvent for PC. V_e or the solubility of CO_2 in THF increases with pressure of CO_2, as is shown clearly in Figures 2 and 4. The solvent power of the solvent should change with the concentration of CO_2 in the solution. In other words, the solvent power is a function of the solubility of CO_2. How the dissolved CO_2 affects the solvent power of the solvent and the conformation, shape, and microstructure of the PC chain in the solution is discussed in the following.

Radii of Gyration and the Second Virial Coefficient. Small-angle X-ray scattering from dilute polymer solution is described by[34]

$$\frac{KC}{I(q,C)} \approx \frac{1}{M_w}\left(1 + \frac{q^2\langle R_g^2\rangle}{3}\right) + 2A_2C \qquad (1)$$

where K is the instrument constant which is related with the electron density; A_2, $\langle R_g^2\rangle^{1/2} \equiv R_g$, C, and M_w stand respectively for the second virial coefficient, the radius of gyration, the concentration of the polymer in the solution, and the weight-average molecular weight. We determined K by using scattering data using the reported method.[30] Once K is known, the SAXS data can be analyzed by the Zimm plot to determine R_g and A_2.

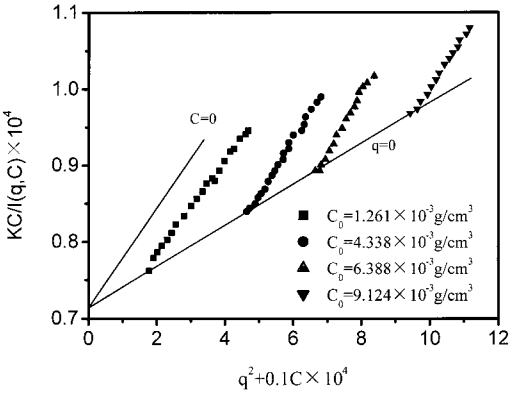

Figure 5. Typical Zimm plot of sample PC-1 at antisolvent pressure of 0.5 MPa.

Table 1. Properties of PC at 308.15 K and Different Antisolvent CO_2 Pressures

samples	$M_w \times 10^{-4}$ (g/mol)	press. (MPa)	$\langle R_g^2\rangle^{1/2}$ (Å)	$A_2 \times 10^4$ (cm^3 mol/g^2)
PC-1[a]	1.4	0	53.0[a]	9.05[a]
PC-1	1.4	0	52.8	8.93
PC-1	1.4	0.5	52.4	6.75
PC-1	1.4	1.0	51.3	4.43
PC-1	1.4	1.5	49.1	3.01
PC-1	1.4	2.0	45.8	1.24
PC-2[a]	1.8	0	60.9[a]	8.08[a]
PC-2	1.8	0	58.9	8.41
PC-2	1.8	0.5	58.2	6.34
PC-2	1.8	1.0	56.6	4.16
PC-2	1.8	1.5	53.8	2.67
PC-2	1.8	2.0	49.8	1.04
PC-3[a]	2.4	0	71.4[a]	7.10[a]
PC-3	2.4	0	67.3	7.29
PC-3	2.4	0.5	65.7	5.24
PC-3	2.4	1.0	63.3	3.61
PC-3	2.4	1.5	59.6	2.09
PC-3	2.4	2.0	54.9	0.87
PC-4[a]	2.9	0	79.3[a]	6.52[a]
PC-4	2.9	0	73.4	6.08
PC-4	2.9	0.5	71.1	4.02
PC-4	2.9	1.0	68.2	2.28
PC-4	2.9	1.5	63.9	0.79
PC-4	2.9	2.0	58.6	0.097

[a] Calculated by the correlation of the data in ref 35.

As an example, Figure 5 shows the Zimm plot of PC-1 at antisolvent CO_2 pressure of 0.5 MPa, which allows a simultaneous extrapolation to $q = 0$ and $C = 0$ to obtain R_g and A_2, and the results are listed in Table 1. Tsuji et al.[35] reported the A_2 and R_g of PC in the solvent THF at 298.15 K determined by the light scattering method in the molecular weight range from 8.35×10^4 to 46.3×10^4 g/mol. The A_2 and R_g can be correlated very well by the equations $A_2 = 0.0665M_w^{-0.451}$ and $R_g = 0.2701M_w^{0.553}$. The values of A_2 and R_g calculated from these two equations are also listed in Table 1. The results determined in this work agree reasonably with the calculated values, as shown in Table 1.

A_2 is directly related with the solvent power of the solvent for the polymers. The larger the A_2 is, the stronger the solvent power. Figure 6 shows the plots of A_2 vs the pressure of CO_2 for polymers of different molecular weights. A_2 decreases with increasing the pressure or solubility of CO_2, which indicates that the solvent power of THF to PC decreases with the concentration of CO_2 in the solution. The results in Figure 6 also indicates that the A_2 decreases with increasing M_w of the polymer; i.e., the PC with lower M_w is more soluble in THF or the mixed solvent.

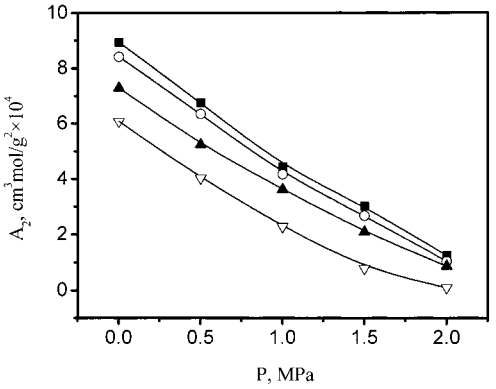

Figure 6. Antisolvent CO_2 pressure dependence of A_2 for PC samples with different molecular weights.

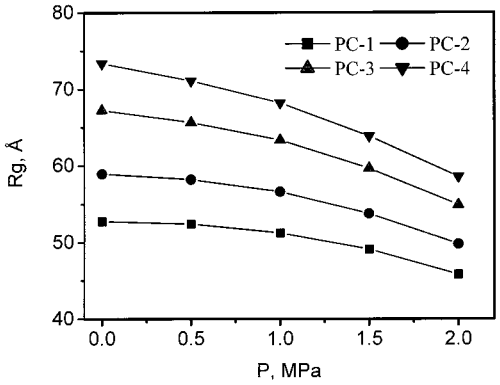

Figure 7. Antisolvent CO_2 pressures dependence of R_g for PC samples with different molecular weights.

R_g is related to the size and conformation of the polymer in the solution. Figure 7 shows dependence of R_g on antisolvent CO_2 pressure for the four samples. The R_g decreases with increasing the antisolvent pressure. It indicates that the PC chain shrinks in the course of adding antisolvent CO_2. The main reason is that the solubility or concentration of antisolvent CO_2 in the solution increases with pressure, as shown clearly in Figure 4. Thus, the solvent power of the solvent or A_2 decreases with pressure of CO_2, as illustrated by Figure 6. THF is a good solvent for PC, and the coil is expanded due to prevailing intersegmental repulsion; after adding CO_2, the solvent power of the solvent is reduced, and PC chain is shrunk due to prevailing intersegmental attraction.

Fractal Behavior of PC Chain in GAS Process. The concept of fractal geometry is an useful tool to describe the polymer structure.[36−39] The M_w of the polymer chain is related to the radius of gyration R_g by $M_w \propto R_g^{d_R}$, where d_R is the fractal dimension in terms of the scaling relationship between mass and the radius of gyration.[40] Figure 8 shows double-logarithmic plots of the radius of gyration R_g vs their weight-average molar mass (M_w) at different antisolvent CO_2 pressures. Figure 8 demonstrates clearly that M_w can be scaled to R_g at different antisolvent CO_2 pressures, and the values of the slope (d_R) are listed in Table 2, which indicates that the PC chains have a fractal structure with a dimension of $d_R = 2.17-2.95$.

Further information about the structure of polymer chain can be obtained from the particle scattering factor $P(q)$, which describes the angular distribution of the scattered light. The SAXS function can be expressed as a product of the particle scattering factor $P(q)$ and the

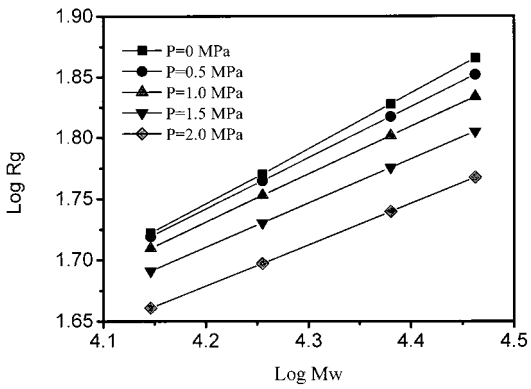

Figure 8. Double-logarithm plots of R_g vs M_w at different antisolvent pressures.

Table 2. Variation of Fractal Dimension with Antisolvent Pressure

press. (MPa)	d_R	d_f	press. (MPa)	d_R	d_f
0	2.17	2.14	1.5	2.74	2.70
0.5	2.38	2.35	2.0	2.95	2.92
1.0	2.56	2.53			

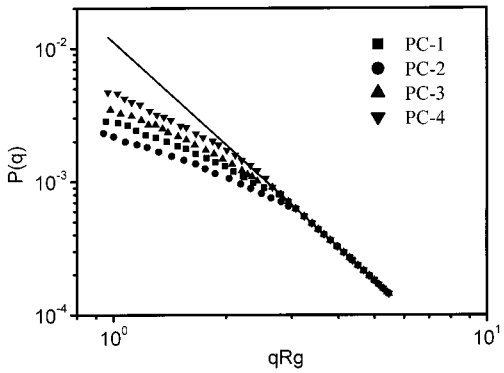

Figure 9. Typical double-logarithm plot of $P(q)$ vs qR_g for four PC samples at antisolvent pressure of 1.0 MPa.

interparticle structure factor $S(q)$ which arises from the interaction between different polymer chains:[41]

$$I(q) = KP(q)\,S(q) \qquad (2)$$

The particle structure factor $P(q) = I(q)/I(0)$ was plotted against the product of the scattering vector q and R_g on a double-logarithmic scale. As an example, the $P(q)$ for the four polymer samples with different molecular weights at antisolvent CO_2 pressure of 1 MPa is plotted against the dimensionless parameter qR_g in Figure 9. The various curves can be contracted into one master curve at $\log(qR_g) > 0.5$. Such a master curve is expected for "self-similar" structures, and power law behavior is observed.[42] The asymptotic slope of this curve is $-d_f = -2.56 \pm 0.02$. Very similar behavior was found at other antisolvent CO_2 pressures, but the exponent d_f depends largely on the antisolvent CO_2 pressure, and the results are also given in Table 2. The exponent d_f of PC chain increases with pressure of antisolvent CO_2.

These results are a clear indication for self-similar structures, which is frequently called fractals, with the values of $d_f = 2.14$, 2.35, 2.53, 2.70, and 2.92, which are not integers but fractal dimensions. Such fractal dimensions are common for disordered objects and demonstrate self-similar behavior, which is understood as a structure that displays the same behavior and is independent of a length scale. In other words, if two

pieces of different sizes are cut from the polymer chain and the smaller is optically magnified to equal size, then the structures appear indistinguishable.[42] A fractal dimension of 2.17−2.95 is characteristic of a polymer chain that has an internal structure between a hard sphere ($d_f = 3.0$) and a fully swollen randomly coiled macromolecule in a thermodynamically good solvent ($d_f = 2.0$).[43] Since the mass inside the radius of a polymer chain is dependent upon the fractal dimension, the fractal dimension is a measure of the compactness of a polymer chain. The larger the fractal dimension, the more compact the structure, and the lower the fractal dimension, the more open is the structure. As can be seen from Table 2, the fractal dimension increases with increasing antisolvent CO_2 pressure, indicating collapse of polymer chain from a coil to a rather dense globule form in the course of adding antisolvent CO_2.

Conclusion

The SAXS study above reveals some striking features: (1) The solvent power of the solvent decreases during adding antisolvent CO_2; accordingly, the size of PC chain decreases in this process. (2) Power law behavior is obtained for the M_w as a function of the radius of gyration with exponents $d_R = 2.17$, 2.38, 2.56, 2.74, and 2.95 for antisolvent CO_2 pressures of 0, 0.5, 1, 1.5, and 2.0 MPa, respectively. (3) An asymptotic power law behavior is found for the angular dependence of the particle scattering factor $P(q)$ with exponents of $d_f = 2.14$, 2.35, 2.53, 2.70, and 2.92 for antisolvent CO_2 pressures of 0, 0.5, 1, 1.5, and 2 MPa, respectively. (4) The fractal dimension (d_R or d_f) increases with increasing antisolvent CO_2 pressure, indicating collapse of the polymer chain from a coil to a rather dense globule form in the course of adding antisolvent CO_2.

Acknowledgment. This work was supported by Ministry of Science and Technology of China and the National Natural Science Foundation of China (2972-5308). The authors are also very grateful to the referees for their valuable suggestions.

References and Notes

(1) McHugh, M. A.; Krukonis, V. J. *Supercritical Fluids Extraction: Principles and Prantice,* 2nd ed.; Butterworth-Heinemann: Stoneham, MA, 1994; p 189.
(2) Eckert, C. A.; Knutson, B. L.; Debenedetti, P. G. *Nature* **1996**, *383*, 313.
(3) Dixon, D. J.; Johnston, K. P.; Bodmeier, R. A. *AIChE J.* **1993**, *39*, 127.
(4) Gallagher, P. M.; Coffey, M. P.; Krukonis, V. J. *J. Supercrit. Fluids* **1992**, *5*, 130.
(5) Robertson, J.; King, M. B.; Swcille, J. P. K.; Merrifield, D. R.; Buxton, P. C. *Proceedings of the 4th International Symposium on Supercritical Fluids*, 1997; p 47.
(6) Shishikura, A. *Proceedings of the 4th International Symposium on Supercritical Fluids*, 1997; p 51.
(7) Catchpole, O. J.; Hochmann, S.; Anderson, S. R. J. In *High-Pressure Chemical Engineering*; von Rohr, Ph. R., Ch. Trepp, Ch., Eds.; 1996; p 309.
(8) Reverchon, E.; Della Porta, G.; Trolio Di, A.; Pace, S. *Ind. Eng. Chem. Res.* **1998**, *37*, 952.
(9) Reverchon, E.; Della Porta, G.; Sannino, D.; Ciambelli, P. *Powder Technol.* **1999**, *102*, 127.
(10) Reverchon, E. *J. Supercrit. Fluids* **1999**, *15*, 1.
(11) Dixon, D. J.; Johnston, K. P. *J. Appl. Polym. Sci.* **1993**, *50*, 1929.
(12) Lele, A.; Shine, A. D. *AIChE J.* **1992**, *38*, 742.
(13) Mawson, S.; Johnston, K. P.; Betts, D. E.; McClain, J. B.; DeSimone, J. M. *Macromolecules* **1997**, *30*, 71.
(14) Luna-Barcenas, G.; Kanakia, S. K.; Sanchez, I. C.; Johnston, K. P. *Polymer* **1995**, *36*, 3173.
(15) Yeo, S.-D.; Debenedetti, P. G.; Radosz, M.; Giesa, R.; Schmidt, H.-W. *Macromolecules* **1995**, *28*, 1316.
(16) Yeo, S.-D.; Debenedetti, P. G.; Radosz, M.; Schmidt, H.-W. *Macromolecules* **1993**, *26*, 6207.
(17) Dixon, D. J.; Luna-Barcenas, G.; Johnston, K. P. *Polymer* **1994**, *35*, 3998.
(18) Luna-Barcenas, G.; Kanakia, S. K.; Sanchez, I. C.; Johnston, K. P. *Polymer* **1995**, *36*, 3173.
(19) Tuminello, W.; Dee, G. T.; McHugh, M. A. *Macromolecules* **1995**, *28*, 1506.
(20) Hayashi, H.; Hamada, F.; Nakajima, A. *Macromolecules* **1974**, *7*, 959.
(21) Konishi, T.; Yoshizaki, T.; Saito, T.; Einaga, Y.; Yamakawa, H. *Macromolecules* **1990**, *23*, 290.
(22) Koyama, H.; Yoshizaki, T.; Einaga, Y.; Hayashi, H.; Yamakawa, H. *Macromolecules* **1991**, *24*, 932.
(23) Abe, F.; Einaga, Y.; Yoshizaki, T.; Yamakawa, H. *Macromolecules* **1993**, *26*, 1884.
(24) Klucker, R.; Schosseler, F. *Macromolecules* **1997**, *30*, 4228.
(25) Beaucage, G. *J. Appl. Crystallogr.* **1995**, *28*, 717.
(26) Chu, B.; Wu, Q. *Macromolecules* **1988**, *21*, 1729.
(27) Pekala, R. W.; Schaefer, D. W. *Macromolecules* **1993**, *26*, 5487.
(28) Venkatraman, A.; Boateng, A. A.; Fan, L. T.; Walawender, W. P. *AIChE J.* **1996**, *42*, 2014.
(29) Schulz, G. V.; Horbach, A. *Makromol. Chem.* **1959**, *29*, 93.
(30) Li, D.; Liu, Z. M.; Han, B. X.; Yang, G. Y.; Wu, Z. H.; Liu, Y.; Dong, B. Z. *Macromolecules* **2000**, *33*, 7990.
(31) Li, D.; Liu, Z. M.; Yang, G. Y.; Han, B. X.; Yan, H. K. *Polymer* **2000**, *41*, 5707.
(32) Lu, J.; Han, B. X.; Yan, H. K. *Phys. Chem. Chem. Phys.* **1999**, *1*, 449.
(33) Dong, B. Z.; Sheng, W. J.; Yang, H. L.; Zhang, Z. J. *J. Appl. Crystallogr.* **1997**, *30*, 877.
(34) Zimm, B. H. *J. Chem. Phys.* **1948**, *16*, 1093.
(35) Tsuji, T.; Norisuye, T.; Fujita, H. *Polym. J.* **1975**, *7*, 558.
(36) Mandelbrot, B. B. *Fractals, Form, Chance and Dimension*; Freeman: San Francisco, 1977.
(37) Mandelbrot, B. B. *The Fractal Geometry of Nature*; Freeman: New York, 1982.
(38) Sander, L. M. *Nature* (*London*) **1986**, *322*, 789.
(39) Sander, L. M. *Sci. Am.* **1986**, *256*, 94.
(40) Stanley, H. E. *J. Phys. A: Math. Gen.* **1977**, *A10*, L211.
(41) Glatter, G.; Krathy, O. *Small-Angle X-ray Scattering*; Academic Press: London, 1982; p 387.
(42) Hanselmann, R.; Burchard, W.; Ehrat, M.; Widmer, H. M. *Macromolecules* **1996**, *29*, 3277.
(43) Stauffer, D.; Coniglio, A.; Adam, M. *Adv. Polym. Sci.* **1982**, *44*, 103.

MA001671K